arXiv:1409.1405v1 [cond-mat.str-el] 4 Sep 2014

A Quantum Fidelity Study of the Anisotropic Next-Nearest-Neighbour Triangular Lattice Heisenberg Model

Mischa Thesberg[1] and Erik S. Sørensen[1,*]

[1]*Department of Physics & Astronomy, McMaster University*
1280 Main St. W., Hamilton ON L8S 4M1, Canada.

(Dated: September 5, 2014)

Ground- and excited-state quantum fidelities in combination with generalized quantum fidelity susceptibilites, obtained from exact diagonalizations, are used to explore the phase diagram of the anisotropic next-nearest-neighbour triangular Heisenberg model. Specifically, the $J' - J_2$ plane of this model, which connects the $J_1 - J_2$ chain and the anisotropic triangular lattice Heisenberg model, is explored using these quantities. Through the use of a quantum fidelity associated with the first excited-state, in addition to the conventional ground-state fidelity, the BKT-type transition and Majumdar-Ghosh point of the $J_1 - J_2$ chain ($J' = 0$) are found to extend into the $J' - J_2$ plane and connect with points on the $J_2 = 0$ axis thereby forming bounded regions in the phase diagram. These bounded regions are then explored through the generalized quantum fidelity susceptibilities χ_ρ, χ_{120°, χ_D and χ_{CAF} which are associated with the spin stiffness, 120° spiral order parameter, dimer order parameter and collinear antiferromagnetic order parameter respectively. These quantities are believed to be extremely sensitivity to the underlying phase and are thus well suited for finite-size studies. Analysis of the fidelity susceptibilities suggests that the $J', J_2 \ll J$ phase of the anisotropic triangular model is either a collinear antiferromagnet or possibly a gapless disordered phase that is directly connected to the Luttinger phase of the $J_1 - J_2$ chain. Furthermore, the outer region is dominated by incommensurate spiral physics as well as dimer order.

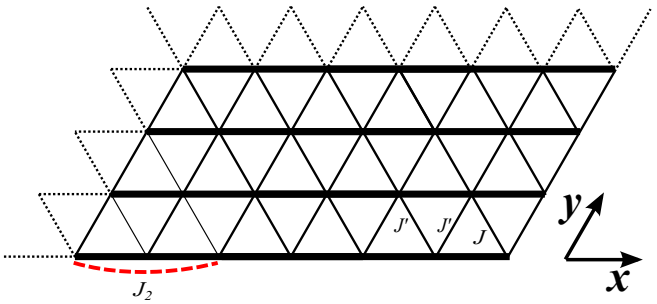

FIG. 1. The anisotropic triangular lattice with next-nearest neighbour interactions. In this paper J' and J_2 are assumed to be ratios of J (i.e. $J = 1$). In the limit $J' \ll 1$ the system can be viewed as a set of weakly coupled chains. The next-nearest neighbour interactions J_2 are in the intra-chain direction (red dashed line). A system size is denoted as $N = W \times L$ corresponding to a system of W chains of length L. The system size studied here is 4×6.

I. INTRODUCTION

The study of quantum phase transitions (QPTs), especially those which occur in two- and one-dimensional systems, remains one of the most active areas of research in condensed matter physics.[1] Of particular interest are systems with competition between interactions that cannot be mutually satisfied. This behaviour, often arising from *frustration*, acts to erode the tendency towards classical orderings and promotes exotic phases dominated by quantum fluctuations. Unfortunately, these quantum fluctuations manifest as highly oscillatory, fermionic field theories. Such theories cause Quantum Monte-Carlo (QMC) methods, numerical methods which allow the study of some of the largest system sizes that are accessible computationally, to fail. In contrast, Exact Diagonalization (ED) methods, that we employ here, are not affected by the presence of frustration and can quite generally be applied to lattice models with a finite Hilbert space. They are, however, restricted to very small system sizes. The use of complimentary methods such as the Density Matrix Renormalization Group (DMRG) and related methods are therefore also extremely valuable and DMRG results for two-dimensional triangular lattice models have already been obtained[2]. However, our focus here is on the information that can be extracted from ED results in combination with new insights arising from the field of quantum information.

The numerical identification of QPTs and the classification of their adjoining quantum phases often involves some *a priori* knowledge about the ordering of the system and the evaluation of quantities, such as the spin stiffness or order parameter, which may have poor behaviour or slow/subtle divergences in small finite systems. A relatively new quantity, with its origin in the field of quantum information, has shown promise as a useful numerical parameter for characterizing QPTs; the quantum fidelity and quantum fidelity susceptibility.[3–6] These quantities have already been successfully employed towards the identification of QPTs in a number of systems,[7–31] and an excellent review of this approach can be found in Ref. 32. In this paper we will be concerned with attempts to slightly generalize the notion of the standard fidelity in order to construct new quantities that can aid in identifying phase transitions in small systems. Extensions of the basic fidelity concept are not new, with prior developments such as the operator fidelity susceptibility[33] and the reduced fidelity[34–36] having proved fruitful. Here

we consider two additional variants that have been proposed: excited-state fidelities[37] and generalized fidelity susceptibilities[38,39]

The typical quantum fidelity assumes that the Hamiltonian of a system with a QPT can be written in the form

$$H(\lambda) = H_0 + \lambda H_\lambda, \tag{1}$$

where the phase transition occurs at some critical value of the *driving parameter* λ (λ_c). From this perspective the second term is then seen as the *driving term* and it is entirely responsible for the phase transition. The quantum fidelity is then defined as the overlap or inner-product of the ground-state of a system with another ground-state determined by a Hamiltonian that is slightly perturbed in the driving parameter relative to the first:

$$F_0(\lambda, \delta\lambda) = \langle \Psi_0(\lambda) \, | \Psi_0(\lambda + \delta\lambda) \rangle \, , \tag{2}$$

where $\Psi_0(\lambda)$ is the ground-state of the Hamiltonian $H(\lambda)$. In a study by Chen *et al.*[37] of the $J_1 - J_2$ chain, a system we also consider here, it was shown that a fidelity based not on the ground-state but the first excited-state,

$$F_1(\lambda, \delta\lambda) = \langle \Psi_1(\lambda) \, | \Psi_1(\lambda + \delta\lambda) \rangle \, , \tag{3}$$

could be a potentially valuable quantity. Here we call such a fidelity an excited-state fidelity.

From the quantum fidelity one can calculate the quantum fidelity susceptibility, defined as

$$\chi_\lambda = \frac{2(1 - F_0(\lambda)}{\delta\lambda^2}. \tag{4}$$

However, in a previous work[38] it was shown that this definition could be extended by considering other types of perturbations beyond a perturbation in the driving parameter. Specifically, it is often useful to construct generalized fidelity susceptibilities associated with the order parameters of common orderings.[39]

Our goal here is to explore the phase-diagram of the anisotropic next-nearest-neighbor triangular lattice model (ANNTLHM). This model connects the $J_1 - J_2$ chain ($J' = 0$) with the anisotropic triangular lattice Heisenberg model (ATLHM) ($J_2 = 0$). The phase diagram of the ATLHM for $J' \ll 1$ and accordingly of the ANNTLHM for $J', J_2 \ll 1$ has proven exceedingly difficult to determine and it appears that several possible phases *very* closely compete.

The $J_1 - J_2$ chain has the Hamiltonian

$$H_{J_1-J_2} = \sum_{\mathbf{x}} \hat{S}_{\mathbf{x}} \cdot \hat{S}_{\mathbf{x+1}} + J_2 \sum_{\mathbf{x}} \hat{S}_{\mathbf{x}} \cdot \hat{S}_{\mathbf{x+2}} \tag{5}$$

where J_2 is understood to be the ratio ($J_2 = J_2'/J_1'$) of the next-nearest neighbour (J_2') and nearest-neighbour (J_1') interaction constants. It is a system which has been well studied; both through field theoretic approaches,[40,41] and through numerical approaches like exact diagonalization,[42,43] and DMRG.[44,45] These studies have revealed the existence of a rich phase diagram for the $J_2 > 0$ region. For $J_2 < J_2^c \sim 0.241$[42] the system exhibits a disordered Luttinger liquid phase characterized by quasi-long-range order (i.e. algebraic decay of spin-spin correlations) and no excitation gap. At J_2^c an energy gap opens and for $J_2^c < J_2$ dimerization sets in and correlations become short-ranged. At the so called Majumdar-Ghosh (MG) point $J_2^{MG} = J/2$ the ground-state of the system is known exactly and with periodic boundary conditions it is exactly two-fold degenerate even for finite systems, a fact that is important for our study. Slightly away from the MG point the degeneracy is lifted for finite systems with an exponentially small separation between the odd and even combinations of the two possible dimerization patterns. The correlation length of the system reaches a minimum at the MG point.[46] The MG point can also be identified as a *disorder* point marking the onset of incommensurate correlations in real-space occuring for $J_2 > J_{MG}$. The incommensurate effects occuring for $J_2 > J_2^{MG}$ are short-ranged and the system remains dimerized for any finite $J_2 > J_2^c$. Of particular importance to us here is the Luttinger liquid-dimer transition at J_2^c, which is known to be in the BKT universality class and difficult to detect numerically, and the onset of incommensurate correlations at the MG point J_2^{MG}. As we shall show here it is possible to track these points into the $J' - J_2$ plane of the ANNTLHM.

The ATLHM (see Fig. 1) is described by the Hamiltonian

$$H_\Delta = \sum_{\mathbf{x},\mathbf{y}} \hat{S}_{\mathbf{x},\mathbf{y}} \hat{S}_{\mathbf{x}-1,\mathbf{y}} + J' \sum_{\mathbf{x},\mathbf{y}} \hat{S}_{\mathbf{x},\mathbf{y}} \cdot \left(\hat{S}_{\mathbf{x},\mathbf{y+1}} + \hat{S}_{\mathbf{x}-1,\mathbf{y+1}} \right), \tag{6}$$

where, like $H_{J_1-J_2}$, the coupling constant J' is taken to be the ratio of the two exchange constants corresponding to the two different exchange terms. The phase diagram of this system for $J' < 1$ has proven extremely hard to determine and many aspects are still undecided. Early interest in this system was fuelled by initial theoretical and numerical studies[47–49] which suggested the existence of a two-dimensional spin liquid phase for $J' \ll 1$. This was especially exciting since the ATLHM is believed to be an accurate description of a number of real experimental materials, such as: the organic salts $\kappa-(\text{BEDT-TTF})_2\text{Cu}_2(\text{CN})_3$[50–52] and $\kappa-(\text{BEDT-TTF})_2\text{Cu}_2[\text{N}(\text{CN})_2]$;[52] and the inorganic salts Cs_2CuCl_4,[53–57] and Cs_2CuBr_4.[57,58] However, later theoretical studies would suggest that experimental results on Cs_2CuCl_4 could be explained within the paradigm of a less exotic quasi-one-dimensional spin liquid.[59,60] This too gave way to a number of recent renormalization group studies which suggest that the $J' \ll 1$ region is not a spin liquid at all but rather that next-nearest chain antiferromagnetic interactions and order-by-disorder give rise to a collinear antiferromagnetic (CAF) ordering.[61,62] In prior work[63], we have studied this system through the use of twisted boundary conditions which alleviate some

of the finite-size issues associated with incommensurate correlations. The application of twisted boundary conditions suggests the existence of incommensurate spiral ordering for $J' \sim 1$ giving way, after a phase transition, to a new phase dominated by antiferromagnetism albeit with short-range incommensurate spiral correlations. In Ref. 63 a rough thermodynamic limit extrapolation suggested the new phase was gapless, though whether a true collinear antiferromagnetic ordering, as suggested by Balents *et al.*,[61] emerged could not be definitively determined.

Here we are concerned with the application of excited-state fidelity and generalized fidelity susceptibility techniques to the more general Hamiltonian (ANNTLHM) including a next-nearest neighbor coupling along the chains:

$$\begin{aligned} H(J', J_2) = & \sum_{\mathbf{x},\mathbf{y}} \hat{S}_{\mathbf{x},\mathbf{y}} \hat{S}_{\mathbf{x-1},\mathbf{y}} \\ & + J' \sum_{\mathbf{x},\mathbf{y}} \hat{S}_{\mathbf{x},\mathbf{y}} \cdot \left(\hat{S}_{\mathbf{x},\mathbf{y+1}} + \hat{S}_{\mathbf{x-1},\mathbf{y+1}} \right) \\ & + J_2 \sum_{\mathbf{x}} \hat{S}_{\mathbf{x}} \cdot \hat{S}_{\mathbf{x-2}}. \end{aligned} \tag{7}$$

As J', J_2 are varied the ANNTLHM interpolates between the $J_1 - J_2$ chain ($J' = 0$ and the ATLHM ($J_2 = 0$) through the creation of a $J' - J_2$ plane (see Fig. 1). To our knowledge such a general system has only been studied field theoretically[61,62] and is believed to exhibit the CAF order discussed previously for small J' and J_2 before transiting to spiral ordering for large J', small J_2, and dimer ordering for large J_2, small J'. We will now more thoroughly introduce and define the excited-state fidelity and generalized fidelity susceptibilities.

II. EXCITED-STATE FIDELITIES

In the context of the quantum fidelity it is sometimes useful to consider a quantum phase transition as a result of a level crossing in the ground- or excited-states as a function of the driving parameter λ.[32] This is a perspective that has proven useful for the study of a class of one-dimensional models[64] and can be partly motivated by the consideration that quantum phase transitions are the result of sudden reconfigurations of the low-lying energy spectrum of a system.

Motivated by this viewpoint it was shown in Ref. 37 (see also Ref. 42) that the BKT-type transition in the $J_1 - J_2$ can be detected, in finite-systems, by locating a level crossing in the *first* excited-states. Thus, the determination of the transition point at $J_2 \sim 0.24$ was possible by constructing a fidelity, F_1, not of the ground-state but of the first excited-state. Using this excited-state fidelity it was demonstrated[37] that an abrupt drop in F_1 as a result of the excited state level crossing occurs at the BKT transition point. Here, we use the same fidelity to follow the behaviour of this transition as it extends into the $J' - J_2$ plane. We note that, from a numerical perspective, it is considerably more convenient to monitor F_1 rather than the associated level crossing since the latter would require an intricate analysis of several of the low-lying states.

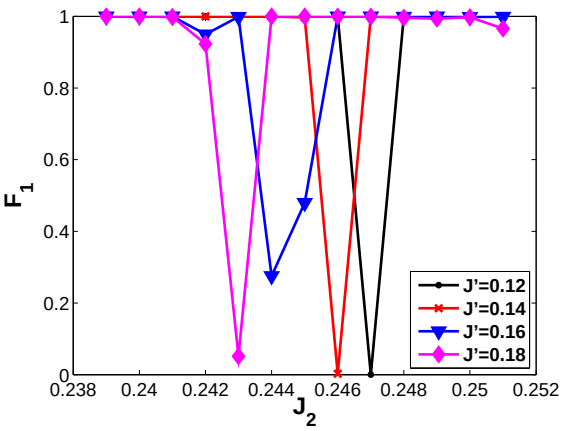

FIG. 2. (Colour available on-line) The first excited-state fidelity vs. J_2 for values of J' of 0.12 (black circles), 0.14 (red crosses), 0.16 (blue triangles) and 0.18 (magenta diamonds). The sharp downward spikes represent a level crossing in the excited state which was shown by Chen *et al.* to signify the BKT-type transition point of the $J_1 - J_2$ chain.[37]

A careful analysis of Ref. 37, specifically Fig. 5 there-in, also indicates the presence of a *ground-state* level crossing at the Majumdar-Ghosh point[65] for finite-systems as mentioned above. This crossing, which occurs where it is known no actual phase transition occurs in the thermodynamic limit, could be detected by the ground-state fidelity (F_0) and coincides with the onset of short-range incommensurate correlations in real space even though no long-range spiral order develops. For a two-dimensional system such as the ATLHM it is known that spiral order occurs close to $J' = 1$ and it is is then also of considerable interest to see if it is possible to track this level crossing through the $J' - J_2$ plane and what bearing, if any, it has on the physics of the ANNTLHM.

To this end, the ground-state and first excited-state of the ANNTLHM were calculated for a 4×6 triangular lattice with periodic boundary conditions using a parallel, Lanczos, exact diagonalization code as outlined by Lin *et al.*[66] Total-S^z symmetry was invoked and numerical errors in ground-state eigenenergies are estimated to be on the order of 10^{-10}. Numerical errors in the first excited-state energies, as is a drawback of the Lanczos method, are considered to be higher by an order of magnitude. It is worth noting that when constructing the excited-state fidelity, and thus solving for the eigenvector of the first excited-state, the difficulty in the Lanczos method of ghost eigenvalue formation is exacerbated and special care must be taken to throw out erroneous results.

Once the ground-state and first excited-state eigenvectors were obtained numerically, F_0 and F_1 were con-

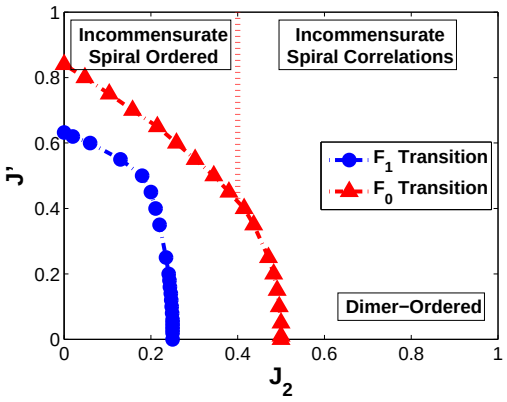

FIG. 3. (Colour available on-line) The phase diagram of the $J'-J_2$ plane of the ANNTLHM with regards to the BKT-type transition of the J_1-J_2 chain, identified by the excited-state fidelity F_1, in blue (circles) and the crossover associated with the onset of short-range incommensurate spiral correlations, identified by F_0, in red (triangles). All results are for a 4×6 system. The dotted red line represents a rough estimate, evidenced by the dimer fidelity susceptibility, of the region where long-range spiral order transitions to short-range incommensurate spiral correlations transition with possible dimer order. It is derived from the data in Fig. 9.

structed as a function of J_2. A typical tracking of the drop in F_1 is shown for various values of J' between 0.12 and 0.18 versus J_2 in Fig. 2. The path of the transition in F_0 is traced in a similar manner. As mentioned above, we calculate F_0, F_1 and therefore only gain indirect information about an assoicate level crossing. However, a further examination of the energy spectrum characteristics which produce the spike in F_0 reveals that it is either due to a ground-state level crossing which persists into the $J'-J_2$ plane or an extremely close avoided level crossing. The resulting phase diagram implied by this finite system is shown in Fig. 3. All results are obtained using a 4×6 system.

One can see that both transitions, when followed, persist well into the $J'-J_2$ plane and ultimately terminate along the $J_2=0$ line. This line corresponds to the ATLHM and it is therefore fruitful to consider their interpretation within the context of that system. However, a thorough consideration with respect to the nearest-neighbour triangular model will be left to section IV, after the introduction of the generalized fidelity susceptibilities. For now it is sufficient to realize that the level-crossing observed at the Majumdar-Ghosh point in the J_1-J_2 chain ultimately connects with the parity transition observed in previous numerical investigations of the ATLHM.[47,48] In Ref. 63 we studied the same system through the use of twisted boundary conditions, which allow a more natural treatment of incommensurate behaviour, and in it was found that, although a transition does occur, this parity transition is an unphysical artefact of a finite-sized system with periodic boundary conditions. The same conclusion was arrived at in the DMRG study of Weichselbaum and White.[2] Thus, it seems that both in the J_1-J_2 chain (where it is known that incommensurate correlations arise past the disorder (MG) point) and in the ANNTLHM this transition may indicate the onset of incommensurate physics.

Using ground-state and excited-state fidelities we have thus demarcated a phase diagram in the $J'-J_2$ plane shown in Fig. 3. It is clear tht the quantities F_0 and F_1 are useful tools for determining the phase diagram. However, equally important as the *location* of QPTs is the nature of the adjacent quantum phases. It is possible to extend the fidelity approach, through the introduction of generalized fidelity susceptibilities, to aid in the identification of the phase in each region that has been found so far. These susceptibilities will now be introduced.

III. GENERALIZED QUANTUM FIDELITY SUSCEPTIBILITIES

In the previous section we showed the simplicity with which quantum phase transitions driven by level crossings, either in the ground-state or low-lying excited-states, can be identified and traced with the quantum fidelity (when generalized to the overlap of excited-states). Once the location of QPTs within phase space have been charted often the next task, when encountering a system of interest, is the identification of the various phase regions. Ideally one would like to be able to associate an order parameter, local or not, with each demarcated phase (or none for a disordered phase).

It has been shown by Zanardi *et al.*[67] and Chen *et al.*[68], that there is a close connection between a fidelity susceptibility and the second derivative of the ground-state energy with respect to the "driving parameter" with which the fidelity susceptibility is constructed:

$$\chi = \sum_n \frac{|\langle\Psi_n|\, H_I\, |\Psi_0\rangle|^2}{\left(E_0(\lambda)-E_n(\lambda)\right)^2},$$

$$\frac{\partial^2 E_0(\lambda)}{\partial\lambda^2} = \sum_n \frac{2\,|\langle\Psi_n|\, H_I\, |\Psi_0\rangle|^2}{\left(E_0(\lambda)-E_n(\lambda)\right)}.$$

As can be seen, the fidelity susceptibility has a higher power in the denominator and is therefore expected to have a higher sensitivity. It is important to note that this relationship holds true even if the "driving" parameter and Hamiltonian (λ and H_λ) are not actually the terms that drive the phase transition. In Ref. 38, it was demonstrated that for the J_1-J_2 chain the different phases can be identified through the use of an appropriately constructed generalized fidelity susceptibility.

When adopting this approach one begins by identifying all the potential phases that one suspects might exist within the phase diagram under study. The primary task is then to construct a fidelity susceptibility for each of these phases which has a similar connection to the order parameter susceptibility of that phase that the regular

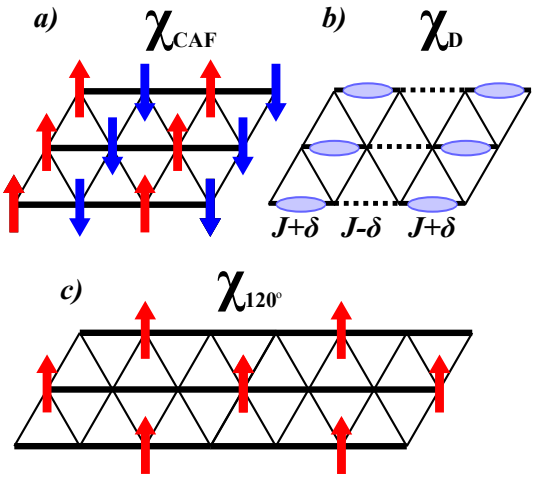

FIG. 4. Diagrams of the perturbing term which define the generalized fidelity susceptibilities χ_{CAF}, χ_D and χ_{120°, respectively. χ_{CAF}, shown in a), is defined by a fidelity whose perturbed Hamiltonian is one with an infinitesimal staggered magnetic field in the S^z direction added according to the illustrated pattern. χ_D, shown in b), is defined by a perturbation in the intra-chain, nearest-neighbour, exchange interaction with alternating bonds having their exchange constant modified by a $\pm\delta$. χ_{120°, shown in c), is a rough probe of spiral order close to that known to exist at $J' = 1, J_2 = 0$ and corresponds to an upward magnetic field on every third site, corresponding to a spiral phase whose ordering has a wavelength of three sites. The omission of in-plane fields on the remaining sites is to maintain the conservation of total-S^z in the system Hamiltonian which improves numerics.

(i.e. λ *is* the driving parameter) fidelity susceptibility has with the ground-state derivatives. It is then expected that such a generalized fidelity susceptibility will exhibit the same behaviour as the order parameter susceptibility, going to infinity when in the associated phase and zero when outside it in the thermodynamic limit, but with increased sensitivity in finite systems.

As has been discussed, the $J_1 - J_2$ chain studied in Ref. 38 serves as a limiting case of the ANNTLHM as $J' \to 0$. Thus, all the fidelity susceptibilities constructed in Ref. 38 find use here, once generalized to two dimensions. To these susceptibilities (χ_ρ, χ_D, χ_{CAF}) have been added the new susceptibility χ_{120° which is designed to capture the incommensurate spiral phase of the $J' \sim 1$ region. We will now explicitly describe the construction of each of these susceptibilities.

1. *The CAF Fidelity Susceptibility, χ_{CAF}*

The collinear antiferromagnetic susceptibility is the natural two-dimensional extension of the antiferromagnetic fidelity susceptibility (χ_{AF}) introduced in Ref. 38. It is constructed by choosing a perturbing Hamiltonian representing a staggered magnetic field which tiles the lattice (See Fig. 4a):

$$\lambda H_{CAF} = \lambda \sum_{\mathbf{y}=0}^{W-1} \sum_{\mathbf{x}=0}^{L-1} (-1)^{\mathbf{x}} S^z_{\mathbf{x},\mathbf{y}}. \tag{8}$$

The generalized fidelity susceptibility associated with this perturbation is then

$$\chi_{CAF} = \frac{2(1 - F(\lambda, J', J_2))}{\lambda^2} \tag{9}$$

where $F(\lambda, J', J_2)$ is given by

$$F(\lambda, J', J_2) = |\langle \Psi_0(0, J', J_2)| \, \Psi_0(\lambda, J', J_2)\rangle| \, . \tag{10}$$

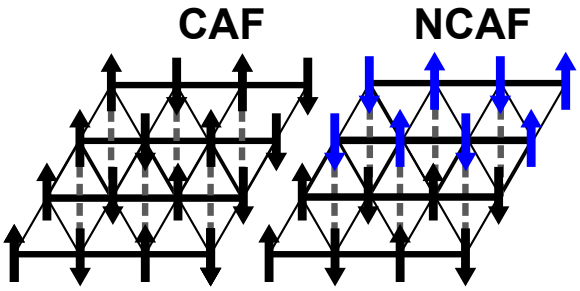

FIG. 5. A diagram comparing the staggered magnetic field arrangement of collinear antiferromagnetic (CAF) vs. non-collinear antiferromagnetic (NCAF) orderings. The key difference is whether next-nearest-chain correlations are antiferromagnetic or ferromagnetic. Field theory work suggests that CAF correlations force an ordered state for $J' \ll 1$.[61] Generalized fidelity susceptibilities were constructed for both CAF and NCAF fields and χ_{CAF} was found to be greater than χ_{NCAF}, though only by a tiny, but meaningful, factor of 0.001%.

As already mentioned, previous work[61–63] on the ANNTLHM has emphasized the important physical difference between antiferromagnetic tilings where next-nearest chain interactions are antiferromagnetic and ferromagnetic as indicated by the dashed lines in Fig. 5. In this work we denote the ferromagnetic case as NCAF (non-collinear antiferromagnetic) ordering and the antiferromagnetic as CAF. Thus, we see that the tiling presented in Fig. 4a is indeed χ_{CAF}. Later we will compare the value of this susceptibility with that for a susceptibility with NCAF ordering, χ_{NCAF}:

$$\lambda H_{NCAF} = \lambda \sum_{\mathbf{y}=0}^{W-1} \sum_{\mathbf{x}=0}^{L-1} (-1)^{\lfloor j/2 \rfloor} S^z_{\mathbf{x},\mathbf{y}} \tag{11}$$

where $\lfloor x \rfloor$ represents the *floor* (i.e. rounded down to the nearest integer) of x. Thus, the additional term switches the ordering every *two* chains and thus produces an NCAF tiling as shown in the right panel of Fig. 5.

The procedure for the calculation of χ_{CAF} then simply amounts to solving for the ground-state of the system

when $\lambda = 0$ and again when λ is some small number. The inner product of the two resulting wave-functions then yields the fidelity. This fidelity is then converted to a susceptibility. We contend that this fidelity susceptibility will have the same properties as the order parameter susceptibility of a collinear-antiferromagnetic phase but with an increased sensitivity, making it more useful for the small system sizes available through ED.

2. The Dimer Fidelity Susceptibility, χ_D

The dimerized susceptibility presented in Ref. 38 is easily extended to two-dimensions. This susceptibility, dictated by the perturbing Hamiltonian

$$\delta H_D = \delta \sum_{\mathbf{y}=0}^{W-1} \sum_{\mathbf{x}=0}^{L-1} (-1)^{\mathbf{x}} S^z_{\mathbf{x},\mathbf{y}} S^z_{\mathbf{x}+\mathbf{1},\mathbf{y}}, \tag{12}$$

corresponds to a dimer tiling *along* chains (here we use δ rather than λ to emphasize the similarity to the classic dimerization operator). One could construct a similar susceptibility which assumes dimerization in the J' direction. However, such a tiling was found to be far less important, this could have been expected *a priori* since the energy benefit of such inter-chain singlet formation is less than that for intra-chain singlets. It is also worth noting that, in principle, one could have two different tilings *with* intra-chain singlets corresponding to a vertical (i.e. along $(0,1)$) and diagonal (i.e. along $(1,1)$) stacking. However, no numerical difference was found between these two possibilities.

As before, a quantum fidelity susceptibility, χ_D is constructed from the fidelity associated with this perturbing Hamiltonian and we take it to be related to the order parameter susceptibility of a dimerized phase.

3. The Spin Stiffness Fidelity Susceptibility, χ_ρ

The spin stiffness is defined as

$$\rho(L) = \left. \frac{\partial^2}{\partial \theta^2} \frac{E_0(\theta)}{L} \right|_{\theta=0} \tag{13}$$

where $E_0(\theta)$ is the ground-state energy as a function of a twist θ applied at every bond:

$$\begin{aligned} H_0 &\rightarrow H_\rho \\ \mathbf{S}_i \cdot \mathbf{S}_j &\rightarrow S^z_i S^z_j + \frac{1}{2}\left(S^+_i S^-_j e^{i\theta} + S^-_i S^+_j e^{-i\theta} \right). \end{aligned} \tag{14}$$

It has proven to be a useful quantity in the exploration of quantum phase diagrams for it can be taken as a measure of the level of spin order exhibited by a phase. In a quasi-long-range ordered system like the Heisenberg chain it is known to take a non-zero value in the thermodynamic limit,[69,70] the same is true for a system with spin ordering. It would be zero in a non-spin ordered system in the thermodynamic limit. The behaviour in finite systems can be less straightforward though it can be said that the sensitivity of a system with respect to an infinitesimal twist can provide valuable information as to the strength of spin-correlations and tendency to order, even in small systems. To benefit from the information stored in a quantity like the spin stiffness while maintaining the sensitivity gains afforded by a fidelity susceptibility we then construct a spin stiffness fidelity susceptibility, χ_ρ. Such a susceptibility is constructed, not by the usual addition of a perturbing conjugate field, but through the transformation Eq. (14) of the system Hamiltonian. One then calculates the overlap of the ground-state of the Hamiltonian with no twist and with an infinitesimal twist in order to construct the appropriate fidelity. Although this does not strictly follow the same form as the other fidelities one could expand the exponential in θ to obtain an $H = H^{(0)} + \theta H^{(1)}_\theta + \theta^2 H^{(2)}_\theta$ form. As is discussed in more detail in Ref. 38, one can then identify $H^{(1)}_\theta$ as a spin current operator and $H^{(2)}_\theta$ as a spin kinetic energy term (see also Ref. 39). However, the numerical difference between the exponential and Taylor expanded forms was found to be negligible and thus in this paper we will merely treat things as an exponential.

We then take the fidelity susceptibility constructed from this spin stiffness fidelity to be a sensitive measure of spin ordering in a probed phase.

4. The 120 Degree Fidelity Susceptibility, χ_{120°

For the isotropic case of $J' = 1$ ($J_2 = 0$) the triangular lattice is known to exhibit a spiral phase with a wavevector of $2\pi/3$ or 120°.[71] As J' becomes less than 1 this spiral order persists, although with incommensurate wavevectors. However, associating a susceptibility with an incommensurate ordering is not feasible without knowledge of the q-vector beforehand. One could invoke estimates of these incommensurate ordering vectors obtained in both the prior studies[2,63] and construct a separate fidelity susceptibility for each value of J'. However, here we employ a simpler, though likely less accurate, approach by defining a generalized fidelity susceptibility for the 120° ordering case only. In the limit of $J' \rightarrow 0$ the classical system will be antiferromagnetically ordered and thus we can expect, in this limit, that χ_{CAF} can correctly identify ordering here. We thus expect a transition from an ordering of wavelength three to an incommensurate ordering with approximate wavelength of two for small systems. Therefore, we can expect a generalized fidelity susceptibility associated with both these limits (i.e. χ_{120° and χ_{CAF}) to provide valuable information about the ordering across the $J_2 = 0$ phase diagram and outwards.

In order to construct χ_{120° an S^z magnetic field is

placed on every third site along a chain (see Fig. 4c) while all other sites were left unaffected. The reason that no magnetic field is placed on the other sites is that the addition of magnetic fields in the $S^x - S^y$ plane would break total-S^z symmetry and significantly complicate numerics. Thus, χ_{120° is constructed in an almost identical fashion to χ_{CAF}, χ_{NCAF} except for the location of the perturbing magnetic fields.

5. *Comparing Generalized Susceptibilities*

The fidelity susceptibilities constructed here are the result of significantly different perturbations with different scaling and absolute magnitude i.e. χ_{CAF} and χ_{NCAF} see the addition of 24 perturbing fields for $N = 4 \times 6$ where as χ_{120° sees only the addition of 8. It is therefore sensible to compare χ_{CAF}, χ_{NCAF} with $3 \times \chi_{120^\circ}$. However, there is no obvious way to quantitatively compare these fidelity susceptibilites to χ_D and χ_ρ for a single system size. Instead a detailed finite-size scaling analysis of the different suceptibilities should be done. For the two-dimensional systems we are considering here it is not possible to perform such a finite-size scaling analysis using ED techniques. In fact, when plotting the susceptibilities arbitrary multiplicative coefficients will be added in front of χ_ρ ($\times 3$) and χ_{120° ($\times 30$) in order to produce graphs with all susceptibilities visible. It is therefore only qualitative comparisons that can be made between these new quantities. However, as we will see, this qualitative behaviour tends to be quite drastic and illuminating and thus provides valuable information about the phase diagram of any system under consideration.

IV. RESULTS AND DISCUSSION

A. The $J_1 - J_2$ Chain ($J' = 0$)

In order to interpret generalized fidelity susceptibility data in the $J' - J_2$ plane it is prudent to begin in the limit where things are well understood. In this system the $J' = 0$ case is such a limit for the system then reduces to the well studied[43–45,72] $J_1 - J_2$ chain. A plot of χ_ρ, χ_D, χ_{CAF} and χ_{120° ($\delta\lambda = 10^{-4}$) is shown in Fig. 6 for a 24 site $J_1 - J_2$ chain as a function of J_2. As such this data amounts to an extension of the data found in Ref. 38.

For $J_2 < 0.2411 = J_2^c$ the system is in the spin-liquid Heisenberg phase marked by quasi-long-range order (i.e. algebraic decay of correlation functions to zero with spin separation), a non-zero spin stiffness,[73,74] and a gapless excitation spectrum. Beyond this phase the system is found to develop a gap for $J_2 > J_2^c$. At the Majumdar-Ghosh point, $J_2 = 1/2 = J_2^{MG}$, the system, in the thermodynamic limit, is a perfect superposition of two dimerized states and the ground-state is known.[65] The MG point is a disorder point and for $J_2 > J_2^{MG}$ incommensurate effects appear in the real-space correlations. The

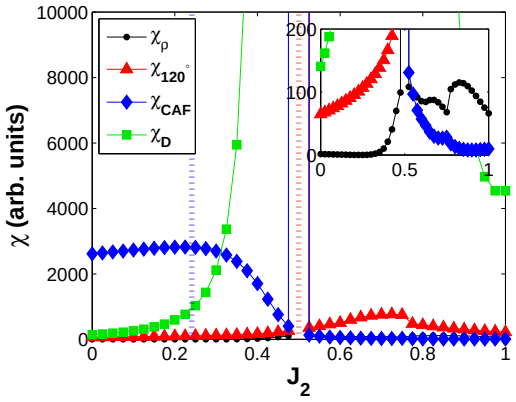

FIG. 6. (Colour available on-line) The values of the generalized fidelity susceptibilities χ_ρ (black circles), χ_{120° (red triangles), χ_{CAF} (blue squares), χ_D (magenta diamonds) as a function of J_2 for $J' = 0$ (i.e. the $J_1 - J_2$ chain). All results are for a 24 site $J_1 - J_2$ chain. Also shown are the locations of the transition detected by the excited-state fidelity F_1 (dotted blue line) and the transition detected by the ground-state fidelity F_0 (dotted red line). χ_ρ has been scaled by a factor of three and χ_{120° has been scaled by a factor of thirty. All other susceptibilities have not been scaled. The inset shows the same data but with a different y-axis.

ability of generalized fidelities to identify and characterize the $J_2 < J_2^{MG}$ region and specifically the $J_2 = J_2^c$ BKT-type transition was established in Ref. 38 and thus that analysis will not be repeated here.

For $J_2 < J_2^c$ the dominant fidelity susceptibility is χ_{CAF}, associated with the antiferromagnetic correlations in the Luttinger phase. (For the $J_1 - J_2$ chain χ_{CAF} used here is identical to χ_{AF} discussed in Ref. 38).

For $J_2 > J_2^c$, χ_{CAF} dramatically decreases while χ_D becomes dominant signalling the onset of dimer order. The distinctive behavior of χ_D for $J_2 > J_2^c$ is reminiscent of the behaviour of the dimer order parameter, whose numerically calculated value can be found in Fig. 5 in Ref. 72 and Fig. 8 in Ref. 45, albeit with increased sensitivity.

Looking at Fig.6 it is also clear that there is an abrupt behavior at $J_2 = 1/2$. It is conspicuous in its; sudden spike and then decay of χ_D; sudden, discontinuous increase in χ_{120° and χ_ρ and; drop and spike of χ_{CAF}. Such behavior is to be expected due to the special 2-fold degenerate ground-state occurring *precisely* at the MG-point for a finite system. For the $J_1 - J_2$ chain this point is the one we previously identified using the fidelity F_0. χ_{120° was constructed as a rough probe of incommensurate or non-antiferromagnetic (i.e. $q \neq \pi$) ordering and for $J_2 > J_2^{MG}$ features develop in χ_{120° consistent with incommensurate (short-range) correlations. For $J_1 - J_2$ chain it is known that *short-range* incommensurate correlations emerge at $J_2 > J_2^{MG}$. It is noteworthy that the generalized fidelity susceptibility has sufficient sensitivity to detect the onset of incommensurability effects be-

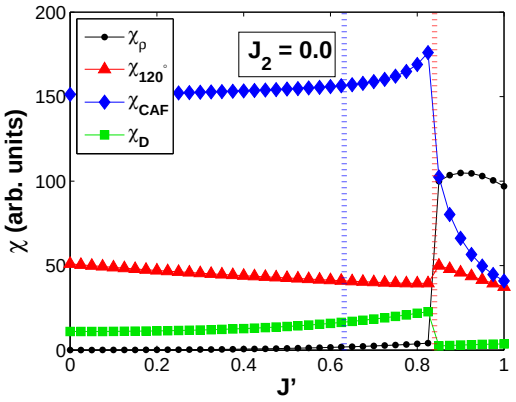

FIG. 7. (Colour available on-line) Generalized fidelity susceptibilities as a function of J' for $J_2 = 0$ (i.e the ATLHM). All marker, line, colour and scaling conventions are the same as those in Fig. 6. Results are for a 4×6 system.

yond the Majumdar-Ghosh point. To summarize, for the $J_1 - J_2$ it is clear that χ_{CAF} and χ_D detect the quasi-AF and dimer order and at the same time the MG point is clearly identifiable with the onset of incommensurability effects.

It is noteworthy that, as was discussed earlier, the MG point of the $J_1 - J_2$ chain is connected, when tracked through the $J' - J_2$ plane, with the unphysical parity transition of the anisotropic nearest-neighbour triangular model. In particular since in the isotropic triangular limit ($J' = 1$, $J_2 = 0$) the system is known to exhibit 120° order and possess no excitation gap. We therefore now turn our attention to the $J_2 = 0$ anisotropic triangular lattice Heisenberg model.

B. The ATHLM ($J_2 = 0$)

A plot of χ_ρ, χ_D, χ_{CAF} and χ_{120° ($\delta\lambda = 10^{-4}$) for $J_2 = 0$ for $J' < 1$ can be found in Fig. 7. It is immediately apparent that there is again a transition, corresponding to the downward spike in F_0 identified earlier, at $J' = 0.840 = J'_c$ and that for $J' < J'_c$, χ_{CAF} and χ_{120° behave in a qualitatively identical manner to the Luttinger phase of the $J_1 - J_2$ chain. On the other hand, χ_D has no spike and simply drops after the transition and although χ_ρ jumps abruptly to a higher value at J'_c, it does not have a minimum anywhere in the $J' < 1$ region.

In Ref. 63 it was shown that the effect of twisted boundary conditions, which allow for incommensurate correlations to exist even in small finite systems, was to change the nature of this J'_c transition from a parity transition to a first-order jump in the ground-state ordering. This jump occurred at a lower J' of 0.765 for $N = 4 \times 6$ and it was observed that incommensurate (short-range) spiral correlations persisted below this new transition though the dominant interaction, and ground-state ordering, was consistent with antiferromagnetism. From the perspective of quantum fidelity susceptibilities used here it is clear that collinear antiferromagentic correlations are very important below the transition point, $J' < J'_c$. However, from the quantum fidelity susceptibilities alone we cannot rule at the existence of a disordered state similar in character to that found in the $J_1 - J_2$ chain for $J_2 < J_2^c$. We now turn to our results for the generalized quantum fidelity susceptibilities in the rest of the $J' - J_2$ plane (i.e. $J' \neq 0$, $J_2 \neq 0$) for the ANNTLHM.

C. The ANNTLHM ($J_2 = 0$)

The same data gathered for the $J_1 - J_2$ chain in Fig. 6 is shown in Fig. 8 for the cases of $J' = 0.2$, 0.4, 0.6 and 0.8. These plots then serve to divide the $J' - J_2$ plane into cross-sections in J'. Again, the point identified by F_0 is clearly visible. Of note in these plots is the consistent behaviour of χ_ρ, χ_{120° and χ_{CAF} as J' increases lending evidence to the notion that the $J' < J'_c$ phase is directly related to the $J_2 < J_2^c$ phase. The one marked difference is in the behaviour of χ_D whose peaked nature becomes substantially less pronounced as J' grows. This is indicative of a necessary (since they have different symmetries) transition from dimer to spiral order. Unfortunately, there does not seem to be sudden features in χ_D vs. J_2 to identify this region. A plot of χ_D vs. J' for J_2s of 0.3 to 0.45 shown in Fig. 9 does suggest a qualitative change in the way χ_D diverges at a J_2 of approximately 0.4. For $J_2 > 0.4$ the peak is much more pronouced than for $J_2 < 0.4$. This could suggest a transition from gapped dimer order with incommensurate short-ranged spiral correlations to the true incommensurate spiral order. In Fig. 3 this is indicated as the dotted red line.

As already stressed, the central observation to make from the results presented in Fig. 8 for $J', J_2 \ll 1$ is the similarity with the results in Fig. 6 for $J_2 < J_2^c$. The presence of a non-zero J' thus only changes the ordering in a very subtle way and possibly not at all.

D. Non-collinear Versus Collinear Order (χ_{NCAF} vs. χ_{CAF})

A final issue of interest is the competition between non-collinear and collinear antiferromagnetic correlations in the anisotropic nearest-neighbour triangular lattice. Renormalization group studies[61,62] of the triangular system suggest that the $J' \ll 1$ phase is ordered antiferromagnetically and that crucial to this ordering is the emergence of antiferromagnetic correlations between *next-nearest chains*. In Ref. 63 it was found that, although next-nearest chain interactions were indeed of great importance within that phase, there is intense competition between collinear (CAF) and non-collinear (NCAF) ordering and that CAF is indeed the dominant correlation, but only by an extremely small margin. To re-investigate this claim a separate generalized fidelity, χ_{NCAF}, was

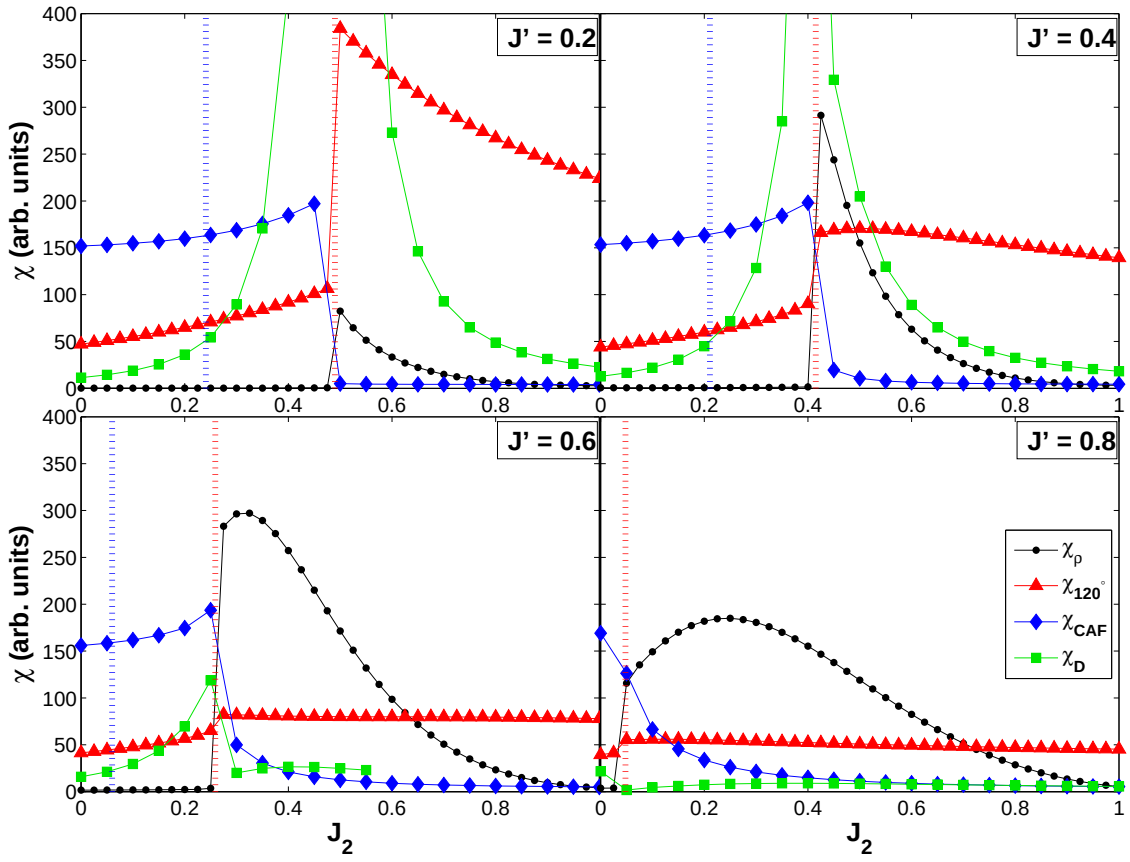

FIG. 8. Generalized fidelity susceptibilities as a function of J_2 for values of $J' = 0.2$, 0.4, 0.6 and 0.8 (i.e. cross-sections of the $J' - J_2$ plane). All marker, line, colour and scaling conventions are the same as those in Fig. 6. Results are for a 4×6 system.

constructed such that next-nearest chains have ferromagnetic interactions and the two (χ_{CAF} and χ_{NCAF}) were computed for $J_2 = 0$, $J' < 1$. The field defining χ_{NCAF} is shown in Fig. 4. As was the case in Ref. 63 the difference between the two is found to be extremely small but χ_{CAF} is larger by a factor of approximately 0.001%. This minuscule discrepancy, though well within the realm of numerical precision, suggests that the competition between these two types of antiferromagnetic correlations is extremely fierce, at least within finite-size systems.

V. CONCLUSION

In this paper the ground-state and excited-state quantum fidelities were used to track the behaviour of the MG/Lifshitz point and BKT-type transition, found in the $J_1 - J_2$ ($J' = 0$) chain, into the $J' - J_2$ plane. It was found that both points trace bounded regions within $J' - J_2$ plane and ultimately terminate on the J' axis ($J_2 = 0$) corresponding to the anisotropic triangular Heisenberg model. Specifically, the MG point, which occurs as a ground-state level crossing in the $J_1 - J_2$ chain which is known to not survive in the thermodynamic limit, is connected to the unphysical parity transition observed in the $J' < 1$ region of the anisotropic triangular model. However, the region defined by the behavior of F_1 connecting the BKT transition of the $J_1 - J_2$ chain ($J' = 0$) with a point on the J' axis is strongly suggestive of a new distinct phase.

In order to further explore and identify these phase regions, the generalized fidelity susceptibilities χ_ρ, χ_{120°, χ_D and χ_{CAF} were constructed. They are associated with the spin stiffness, 120° spiral phase order parameter, dimer order parameter and collinear antiferromagnetic order parameter respectively. These quantities are believed to be very sensitive and therefore well suited for finite system studies.

When plotting these quantum fidelity susceptibilities within the $J' - J_2$ plane the region defined by F_0 is readily identifiable while the F_1 region is much more subtle. In the $J', J_2 \ll 1$ region the χ_{CAF} is marginally favored over

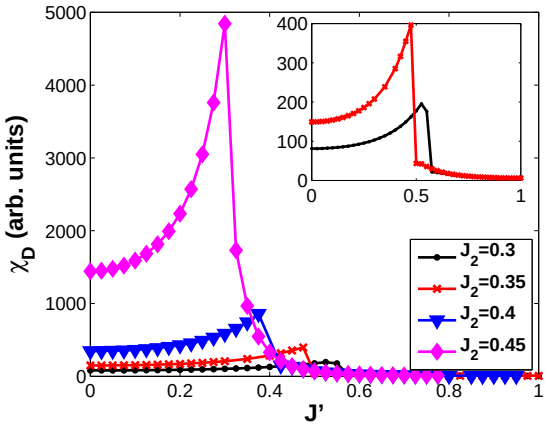

FIG. 9. χ_D as a function of J' for $J_2 = 0.3$ (black circles), 0.35 (red crosses), 0.4 (blue triangles) and 0.45 (magneta diamonds). The inset shows the same data for only $J_2 = 0.35$ and 0.3. A qualitative change in the nature of χ_D can be seen at $J_2 \sim 0.4$. For $J_2 > 0.4$ the peak in χ_D is significantly more pronouced. This could suggest a transition from gapped dimer order with incommensurate short-ranged spiral correlations to the true incommensurate spiral order that exists at $J' = 1, J_2 = 0$.

χ_{NCAF} but it is not possible to conclusively eliminate the possibility of a disordered phase. Furthermore, the region above this phase (i.e. $J_2 > J_2^c$, $J' > J'_c$) is spiral ordered within a $N = 4 \times 6$ system. This is known to be the case in the thermodynamic limit for the anisotropic nearest-neighbour triangular model but for the $J_1 - J_2$ chain this is known to be false and for J_2 beyond the MG point incommensurate correlations are only short-ranged for the $J_1 - J_2$ chain. For J_2 greater than approximately 0.4 dimer correlations appear dominant. A possible way to distinguish these two phases would be through a study of larger system sizes (like those done by Weichselbaum and White in Ref. 2) to track the closure of the energy-gap in the incommensurate phase of the $J_1 - J_2$ chain as that phase connects with the spiral-ordered phase of the triangular lattice through the $J' - J_2$ plane.

An additional aspect not explored in this paper, due to the lack of available system sizes, is the scaling behaviour of these generalized fidelity susceptibilities throughout the $J' - J_2$ plane. Such a study, potentially viable through DMRG of a finite-cluster, would be very valuable and further solidify the understanding of this phase diagram.

ACKNOWLEDGMENTS

The authors would like to thank Sung-Sik Lee, Catherine Kallin and Sedigh Ghamari for many fruitful discussions. We also acknowledge computing time at the Shared Hierarchical Academic Research Computing Network (SHARCNET:www.sharcnet.ca) and research support from NSERC.

* thesbeme@mcmaster.ca

1 S. Sachdev, *Quantum Phase Transitions* (Cambridge University Press, 2011).
2 A. Weichselbaum and S. R. White, Phys. Rev. B **84**, 245130 (2011).
3 H. T. Quan, Z. Song, X. F. Liu, P. Zanardi, and C. P. Sun, Phys. Rev. Lett. **96**, 140604 (2006).
4 P. Zanardi and N. Paunković, Phys. Rev. E **74**, 031123 (2006).
5 H.-Q. Zhou and J. P. Barjaktarevi, Journal of Physics A: Mathematical and Theoretical **41**, 412001 (2008).
6 W.-L. You, Y.-W. Li, and S.-J. Gu, Phys. Rev. E **76**, 022101 (2007).
7 P. Zanardi, M. Cozzini, and P. Giorda, Journal of Statistical Mechanics: Theory and Experiment **2007**, L02002 (2007).
8 M. Cozzini, P. Giorda, and P. Zanardi, Phys. Rev. B **75**, 014439 (2007).
9 M. Cozzini, R. Ionicioiu, and P. Zanardi, Phys. Rev. B **76**, 104420 (2007).
10 P. Buonsante and A. Vezzani, Phys. Rev. Lett. **98**, 110601 (2007).
11 L. Campos Venuti, M. Cozzini, P. Buonsante, F. Massel, N. Bray-Ali, and P. Zanardi, Phys. Rev. B **78**, 115410 (2008).
12 D. Schwandt, F. Alet, and S. Capponi, Phys. Rev. Lett. **103**, 170501 (2009).
13 A. F. Albuquerque, F. Alet, C. Sire, and S. Capponi, Physical Review B **81**, 064418 (2010).
14 W. W. Cheng and J.-M. Liu, Phys. Rev. A **82**, 012308 (2010).
15 M. Thakurathi, D. Sen, and A. Dutta, Phys. Rev. B **86**, 245424 (2012).
16 B. Damski, Phys. Rev. E **87**, 052131 (2013).
17 Y. Nishiyama, Phys. Rev. E **88**, 012129 (2013).
18 W.-L. You and Y.-L. Dong, Phys. Rev. B **84**, 174426 (2011).
19 V. Mukherjee and A. Dutta, Phys. Rev. B **83**, 214302 (2011).
20 B. Wang, M. Feng, and Z.-Q. Chen, Phys. Rev. A **81**, 064301 (2010).
21 W.-C. Yu, H.-M. Kwok, J. Cao, and S.-J. Gu, Phys. Rev. E **80**, 021108 (2009).
22 S.-J. Gu, H.-M. Kwok, W.-Q. Ning, and H.-Q. Lin, Phys. Rev. B **77**, 245109 (2008).
23 K.-W. Sun and Q.-H. Chen, Phys. Rev. B **80**, 174417 (2009).
24 B. Li, S.-H. Li, and H.-Q. Zhou, Phys. Rev. E **79**, 060101 (2009).
25 A. Tribedi and I. Bose, Phys. Rev. A **77**, 032307 (2008).
26 B. Wang, M. Feng, and Z.-Q. Chen, Phys. Rev. A **81**, 064301 (2010).
27 N. T. Jacobson, S. Garnerone, S. Haas, and P. Zanardi, Phys. Rev. B **79**, 184427 (2009).
28 Y.-C. Li and S.-S. Li, Phys. Rev. A **79**, 032338 (2009).

[29] Y. Nishiyama, Physica A: Statistical Mechanics and its Applications **392**, 4345 (2013).
[30] S. Garnerone, D. Abasto, S. Haas, and P. Zanardi, Phys. Rev. A **79**, 032302 (2009).
[31] M.-F. Yang, Phys. Rev. B **76**, 180403 (2007).
[32] S. Gu, International Journal of Modern Physics B **24**, 4371 (2010).
[33] X. Wang, Z. Sun, and Z. D. Wang, Phys. Rev. A **79**, 012105 (2009).
[34] M. Znidaric and T. Prosen, Journal of Physics A: Mathematical and General **36**, 2463 (2003).
[35] H.-Q. Zhou, ArXiv e-prints (2007), arXiv:0704.2945 [cond-mat.stat-mech].
[36] E. Eriksson and H. Johannesson, Phys. Rev. A **79**, 060301 (2009).
[37] S. Chen, L. Wang, S.-J. Gu, and Y. Wang, Phys. Rev. E **76**, 061108 (2007).
[38] M. Thesberg and E. S. Sørensen, Phys. Rev. B **84**, 224435 (2011).
[39] S. Greschner, A. K. Kolezhuk, and T. Vekua, Phys. Rev. B **88**, 195101 (2013).
[40] F. D. M. Haldane, Phys. Rev. B **25**, 4925 (1982).
[41] S. Eggert and I. Affleck, Phys. Rev. B **46**, 10866 (1992).
[42] S. Eggert, Phys. Rev. B **54**, R9612 (1996).
[43] T. Tonegawa and I. Harada, J. Phys. Soc. Jpn. **56**, 2153 (1987).
[44] R. Chitra, S. Pati, H. R. Krishnamurthy, D. Sen, and S. Ramasesha, Phys. Rev. B **52**, 6581 (1995).
[45] S. R. White and I. Affleck, Phys. Rev. B **54**, 9862 (1996).
[46] A. Deschner and E. S. Sørensen, Phys. Rev. B **87**, 094415 (2013).
[47] M. Q. Weng, D. N. Sheng, Z. Y. Weng, and R. J. Bursill, Phys. Rev. B **74**, 012407 (2006).
[48] D. Heidarian, S. Sorella, and F. Becca, Phys. Rev. B **80**, 012404 (2009).
[49] J. Merino, R. H. McKenzie, J. B. Marston, and C. H. Chung, Journal of Physics: Condensed Matter **11**, 2965 (1999).
[50] Y. Shimizu, K. Miyagawa, K. Kanoda, M. Maesato, and G. Saito, Phys. Rev. Lett. **91**, 107001 (2003).
[51] Y. Qi, C. Xu, and S. Sachdev, Phys. Rev. Lett. **102**, 176401 (2009).
[52] H. C. Kandpal, I. Opahle, Y.-Z. Zhang, H. O. Jeschke, and R. Valentí, Phys. Rev. Lett. **103**, 067004 (2009).
[53] R. Coldea, D. A. Tennant, A. M. Tsvelik, and Z. Tylczynski, Phys. Rev. Lett. **86**, 1335 (2001).
[54] O. A. Starykh, H. Katsura, and L. Balents, Phys. Rev. B **82**, 014421 (2010).
[55] R. Coldea, D. A. Tennant, R. A. Cowley, D. F. McMorrow, B. Dorner, and Z. Tylczynski, Phys. Rev. Lett. **79**, 151 (1997).
[56] R. Coldea, D. A. Tennant, K. Habicht, P. Smeibidl, C. Wolters, and Z. Tylczynski, Phys. Rev. Lett. **88**, 137203 (2002).
[57] W. Zheng, R. R. P. Singh, R. H. McKenzie, and R. Coldea, Phys. Rev. B **71**, 134422 (2005).
[58] H. Tanaka, T. Ono, H. A. Katori, H. Mitamura, F. Ishikawa, and T. Goto, Progress of Theoretical Physics Supplement **145**, 101 (2002), http://ptps.oxfordjournals.org/content/145/101.full.pdf+html.
[59] M. Kohno, L. Balents, and O. Starykh, Journal of Physics: Conference Series **145**, 012062 (2009).
[60] L. Balents, Nature **464**, 199 (2010).
[61] O. A. Starykh and L. Balents, Phys. Rev. Lett. **98**, 077205 (2007).
[62] S. Ghamari, C. Kallin, S.-S. Lee, and E. S. Sørensen, Phys. Rev. B **84**, 174415 (2011).
[63] M. Thesberg and E. S. Sorensen, ArXiv e-prints (2014), arXiv:1406.4083 [cond-mat.str-el].
[64] G.-S. Tian and H.-Q. Lin, Phys. Rev. B **67**, 245105 (2003).
[65] C. K. Majumdar, Journal of Physics C: Solid State Physics **3**, 911 (197
[66] H. Q. Lin, Phys. Rev. B **42**, 6561 (1990).
[67] P. Zanardi, P. Giorda, and M. Cozzini, Phys. Rev. Lett. **99**, 100603 (2007).
[68] S. Chen, L. Wang, Y. Hao, and Y. Wang, Phys. Rev. A **77**, 032111 (2008).
[69] B. S. Shastry and B. Sutherland, Phys. Rev. Lett. **65**, 243 (1990).
[70] B. Sutherland and B. S. Shastry, Phys. Rev. Lett. **65**, 1833 (1990).
[71] Z. Weihong, R. H. McKenzie, and R. R. P. Singh, Phys. Rev. B **59**, 14367 (1999).
[72] R. Bursill, G. A. Gehring, D. J. J. Farnell, J. B. Parkinson, T. Xiang, and C. Zeng, Journal of Physics: Condensed Matter **7**, 8605 (1995).
[73] J. Bonča, J. P. Rodriguez, J. Ferrer, and K. S. Bedell, Phys. Rev. B **50**, 3415 (1994).
[74] N. Laflorencie, S. Capponi, and E. S. Sørensen, The European Physical Journal B - Condensed Matter and Complex S